

Evidence for topological superconductivity: Topological edge states in Bi_2Te_3/FeTe heterostructure

Bin Guo(郭斌), Kai-Ge Shi(师凯歌), Hai-Lang Qin(秦海浪), Liang Zhou(周良), Wei-Qiang Chen(陈伟强), Fei Ye(叶飞), Jia-Wei Mei(梅佳伟), Hong-Tao He(何洪涛), Tian-Luo Pan(潘天洛), Gan Wang(王干)

Citation: Chin. Phys. B . 2020, 29(9): 097403 . **doi:** 10.1088/1674-1056/abaf9c
Journal homepage: http://cpb.iphy.ac.cn; http://iopscience.iop.org/cpb

What follows is a list of articles you may be interested in

A simple tight-binding approach to topological superconductivity in monolayer MoS_2

H Simchi

Chin. Phys. B . 2020, 29(2): 027401 . **doi:** 10.1088/1674-1056/ab6552

Different behavior of upper critical field in $Fe_{1-x}Se$ single crystals

Shunli Ni(倪顺利), Wei Hu(胡卫), Peipei Shen(沈沛沛), Zhongxu Wei(魏忠旭), Shaobo Liu(刘少博), Dong Li(李栋), Jie Yuan(袁洁), Li Yu(俞理), Kui Jin(金魁), Fang Zhou(周放), Xiaoli Dong(董晓莉), Zhongxian Zhao(赵忠贤)

Chin. Phys. B . 2019, 28(12): 127401 . **doi:** 10.1088/1674-1056/ab50b4

Superconductivity with peculiar upper critical fields in quasi-one-dimensional Cr-based pnictides

Guang-Han Cao(曹光旱), Zeng-Wei Zhu(朱增伟)

Chin. Phys. B . 2018, 27(10): 107401 . **doi:** 10.1088/1674-1056/27/10/107401

Enhancement of off-state characteristics in junctionless field effect transistor using a field plate

Bin Wang(王斌), He-Ming Zhang(张鹤鸣), Hui-Yong Hu(胡辉勇), Xiao-Wei Shi(史小卫)

Chin. Phys. B . 2018, 27(6): 067402 . **doi:** 10.1088/1674-1056/27/6/067402

Observation of mode-like features in tunneling spectra of iron-based superconductors

Gong Jing, Hou Xing-Yuan, Zhu Jun, Jie Yun-Yin, Gu Ya-Dong, Shen Bing, Ren Cong, Li Chun-Hong, Shan Lei

Chin. Phys. B . 2015, 24(7): 077402 . **doi:** 10.1088/1674-1056/24/7/077402

SPECIAL TOPIC — Topological 2D materials

Evidence for topological superconductivity: Topological edge states in Bi_2Te_3/FeTe heterostructure*

Bin Guo(郭斌)[1], Kai-Ge Shi(师凯歌)[1], Hai-Lang Qin(秦海浪)[1], Liang Zhou(周良)[1], Wei-Qiang Chen(陈伟强)[1], Fei Ye(叶飞)[1], Jia-Wei Mei(梅佳伟)[1], Hong-Tao He(何洪涛)[1], Tian-Luo Pan(潘天洛)[1,†], and Gan Wang(王干)[1,2,‡]

[1] *Shenzhen Institute for Quantum Science and Engineering & Department of Physics, Southern University of Science and Technology, Shenzhen* 518055, *China*
[2] *Guangdong Provincial Key Laboratory of Quantum Science and Engineering, Shenzhen Institute for Quantum Science and Engineering, Southern University of Science and Technology, Shenzhen* 518055, *China*

(Received 13 April 2020; revised manuscript received 29 May 2020; accepted manuscript online 15 August 2020)

Majorana fermions have been predicted to exist at the edge states of a two-dimensional topological superconductor. We fabricated single quintuple layer (QL) Bi_2Te_3/FeTe heterostructure with the step-flow epitaxy method and studied the topological properties of this system by using angle-resolved photoemission spectroscopy and scanning tunneling microscopy/spectroscopy. We observed the coexistence of robust superconductivity and edge states on the single QL Bi_2Te_3 islands which can be potential evidence for topological superconductor.

Keywords: Bi_2Te_3/FeTe heterostructure, topological superconductivity, edge states, scanning tunnelling microcopy

PACS: 74.55.+v, 74.70.Xa, 74.78.−w, 74.78.Fk **DOI:** 10.1088/1674-1056/abaf9c

1. Introduction

Majorana zero modes, with non-Abelian exchange statistics, may pave the way for realizing topological quantum computation.[1] The theoretical study predicts that a topological insulator combined with a superconductor holds promising potential application in searching for Majorana fermions and Majorana zero modes, which can exist not only at the surface states of three-dimensional (3D) systems, but also at the edge states of two-dimensional (2D) systems or one-dimensional (1D) wires.[2–5] Low-dimensional system with less degrees of freedom is undoubted in providing more convenience for our research. Edge states, a typical topological property, have never been found in the boundary of conventional superconductor like Pb.[6,7] Thus, the coexistence of edge modes and superconductivity can be a potential evidence for topological superconductor. So far, many low-dimensional systems have already been built and edge modes have been observed in them. A simple method is combining the superconductor together with some low-dimensional materials in which the edge modes exist intrinsically.[8–11] For example, the coexistence of edge states and superconductivity has been observed on the thin film of bilayers Bi(111) grown on the superconducting $NbSe_2$ substrate.[8] Lüpke *et al.* also observed the proximity-induced superconducting gap in the quantum spin Hall edge state of monolayer WTe_2 placed in proximity with $NbSe_2$.[9] Besides, edge modes have also been observed on some ferromagnetic materials combined with a conventional superconductor with strong spin–orbit interaction. In Fe islands on the Re(0001)-O(2×1) surface, where magnetic Fe is combined with superconducting Re to generate topological superconductor, a full rim like edge state is clearly revealed.[12] Similar edge modes have also been observed at the endpoints of Co chains and Fe chains on Pb.[13,14] Obviously, the study of edge states has been an effective tool for us to search and study new 2D topological superconductors.

In recent years, the Bi_2Te_3/FeTe heterostructure has been reported as a potential topological superconductor. Iron telluride, one kind of iron chalcogenides having been intensively studied in both bulk and film forms, is not superconducting without element doping.[15,16] The other component in this system, bismuth telluride, is a characteristic 3D topological insulator. Neither the FeTe nor the Bi_2Te_3 is superconductive, so the origin of the superconductivity in this heterostructure attracted extensive attention. In 2014, Wang *et al.* first reported the superconductivity in this heterostructure,[17] and then He *et al.* measured the saturated T_C on five quintuple layers (QLs) Bi_2Te_3 by transport experiments.[18] Recently,

*Project supported by the National Natural Science Foundation of China (Grant Nos. 61734008 and 11774143), the National Key Research and Development Program of China (Grant Nos. 2018YFA0307100, 2016YFA0301703, and 2016YFA0300300), the Natural Science Foundation of Guangdong Province, China (Grant Nos. 2015A030313840 and 2017A030313033), the State Key Laboratory of Low-Dimensional Quantum Physics (Grant No. KF201602), Technology and Innovation Commission of Shenzhen Municipality, China (Grant Nos. ZDSYS20170303165926217 and JCYJ20170412152334605), and Guangdong Provincial Key Laboratory, China (Grant No. 2019B121203002). J.-W.M. was partially supported by the Program for Guangdong Introducing Innovative and Entrepreneurial Teams, China (Grant No. 2017ZT07C062).

†Corresponding author. E-mail: wangg@sustech.edu.cn
‡Corresponding author. E-mail: pantl@sustech.edu.cn

© 2020 Chinese Physical Society and IOP Publishing Ltd

via the application of the step-flow epitaxy, we achieved a high-quality van der Waals (vdW) heterojunction with one QL Bi_2Te_3 deposited on the epitaxial FeTe grown on $SrTiO_3$ (STO), showing a high transition temperature around 13 K.[19] Meanwhile, we found the existence of electron transfer from FeTe to Bi_2Te_3 so the hole-doped FeTe may well be the parent of superconductivity. Qwada *et al.* also drew a same conclusion by electronic structure measurement.[20] However, for such a potential topological superconductor, although these studies have yielded good results and put forward a reasonable explanation for the origin of superconductivity, it is still a giant blank in the research about the topological properties.

In this work, we will present our initial attempt in searching for edge states in Bi_2Te_3/FeTe heterostructure and show our preliminary results, leading us to propose that the edge states can be observed on the edge of the superconducting single QL Bi_2Te_3 islands grown on the FeTe terraces. We believe that our results could potentially extend the platform for searching of the edge states to this new Bi_2Te_3/FeTe system, making future search for the Majorana Fermions in such system feasible.

2. Experiment methods

This work was done in a joint-vacuum system, with molecular beam epitaxy (MBE) chamber for epitaxy, and two analytical chambers for carrying out angle-resolved photoemission spectroscopy (ARPES) and scanning tunnelling microscopy/spectroscopy (STM/STS) study. The base vacuum for MBE, ARPES, and STM are 3×10^{-10} mbar, 5×10^{-10} mbar, and 1×10^{-10} mbar, respectively. During the experiment, the high quality Bi_2Te_3/FeTe heterostructures were epitaxially grown on 0.07 wt% Nb-doped STO(100) substrates, using step-flow method as described in a separate paper.[19] In this work, we deposited 0.5 QL Bi_2Te_3 on FeTe, where the 1 QL Bi_2Te_3 islands did not completely cover the FeTe terrace. From STM characterization of several regions, we found that the Bi_2Te_3 coverage is around fifty percent, which we called 0.5 QL Bi_2Te_3. After deposition of about 0.5 QL Bi_2Te_3 on FeTe, the sample was *in-situ* transferred to the analytical chambers for carrying out the electronic structure study. In detail, the *in-situ* ARPES measurements were carried out at around 15 K using a SPECS PHOIBOS 150 hemispherical energy analyzer and a light source from a helium discharge lamp (He I, photon energy 21.218 eV). Then this sample was transferred to an *in-situ* Joule–Thomson (JT) STM for a systematic study. The STM measurement was performed with tungsten tips at 1.1 K. The ARPES measurement was acquired on the whole 0.5 QL Bi_2Te_3/FeTe sample while the STM study was focused on single layer Bi_2Te_3 islands.

3. Results and discussion

3.1. Epitaxy of Bi_2Te_3 on FeTe

High quality Bi_2Te_3/FeTe heterojunction was grown in the MBE chamber first. Figure 1(a) shows the lattice illustration of single layer FeTe and single layer Bi_2Te_3, in which they demonstrate the epitaxial relationship of $(111)_{Bi_2Te_3} \parallel (001)_{FeTe}$, naturally forming a vdW heterostructure. Meanwhile, the plane-view simulation shows the arrangement of superficial Te atoms on FeTe(001) and Bi_2Te_3(111) surfaces, clearly indicating a hexagonal-square mismatch at the heterointerface. During the entire growth process, RHEED patterns of different growth stages were recorded, and are shown in Figs. 1(b)–1(d). Figure 1(b) was acquired from the annealed STO(001) substrate. The surface shows a clear 2×1 reconstruction combining long streaky diffraction, which is crucial for the step-flow epitaxy to overcome the giant mismatch shown in Fig. 1(a).[21] The long streaky RHEED can be kept after the growth of FeTe of 20 nm thickness (Fig. 1(c)), representing an atomically flat (001) surface being grown. In the last deposition of Bi_2Te_3, the RHEED pattern changes to Fig. 1(d) after the deposition of just 1 QL Bi_2Te_3, and remains streaky till the end. In Fig. 1(d), it is worth noting that two sets of diffraction patterns are observed, indicating two types of domains existing in the Bi_2Te_3 film. Line 1 and line 2 are the first order and the second order diffraction fringes of domain #1, while line 3 is the first order diffraction fringe of domain #2. The distance between line 3 and line 0 is $\sqrt{3}$ times of that between line 1 and line 0, which means the domain #1 rotated 30° related to domain # 2, as illustrated in Fig. 1(e). The double-domain feature can be explained by considering

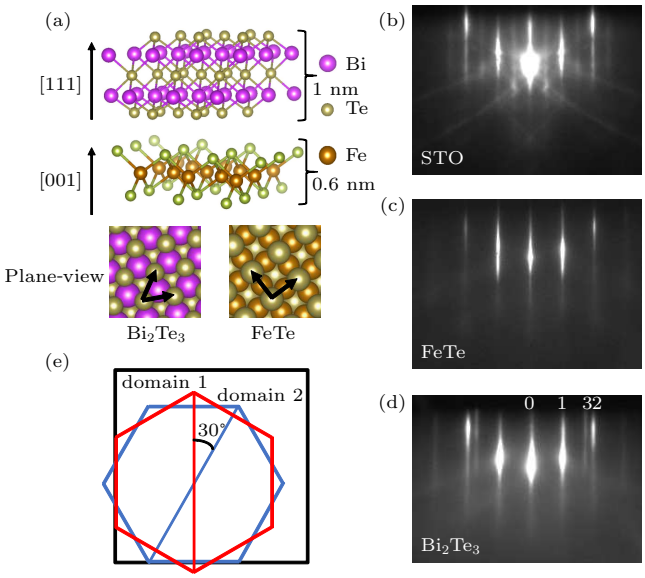


Fig. 1. MBE growth of the Bi_2Te_3 and FeTe films. (a) The schematic crystal structure of Bi_2Te_3 and FeTe. (b) The RHEED pattern of the STO surface which shows that the substrate has a well-defined 2×1 surface reconstruction. (c) The RHEED pattern of the FeTe surface. (d) The RHEED pattern of the Bi_2Te_3 surface. The double-line structure shows two kinds of domains in the Bi_2Te_3 film. (e) Schematic of two types of Bi_2Te_3 crystal domains on FeTe.

the step-flow epitaxy and the symmetric mismatch as shown in Fig. 1(e), which shows two ways of lateral alignment when hexagonal Bi_2Te_3 is connecting with the square FeTe lattice's atomic steps. Nevertheless, all the following STM/STS studies were performed on the 1 QL Bi_2Te_3 island which is small enough for possessing only a single domain, thus the macroscopic rotation freedom does not affect our microscopic electronic states study.

3.2. Electronic structure study

Before carrying out of local electronic study on epitaxial sample using STM, we analyzed the electronic structure evolution depending on the thickness of Bi_2Te_3 step by step. Figure 2(a) is a photoemission intensity map of a cut along the Γ–M direction of FeTe band acquired on as-grown FeTe(001) surface. Figure 2(b) is a cut along the same direction but acquired after the deposition of 0.5 QL Bi_2Te_3. Because of the low Bi_2Te_3 coverage, the photoelectrons detected in Fig. 2(b) were mainly from FeTe. Therefore, the raw data in these two stages look very similar. However, we still can find that the band structure shown in Fig. 2(b) is indeed of subtle differences comparing with Fig. 2(a). To make them clearly, differential intensity maps of Figs. 2(a) and 2(b) are shown in Figs. 2(d) and 2(e), respectively. The EDC mapping of Fig. 2(b) is also displayed in Fig. 2(c). In both Figs. 2(c) and 2(e), three individual bands, labeled as bands α, β, and γ, are remarkably distinguished. Among them, the band α also appears in pure FeTe's Fermi surface as shown in Fig. 2(d). Comparing with previous report about FeTe's band structure,[22] we find this band crossing the Fermi level is a characteristic feature of FeTe band, indicating the hole pocket near the Γ point. The band β is a flat band that was also reported belonging to FeTe obtained at 88 K,[23] however, its energy level and appearing temperature here are different, since we performed the experiment at 15 K. Till now, the search for the origin of band β is still undergoing, which will be discussed in a separate report. Hereby we want to pay more attention on the band γ. Via the literature survey, we find no band like the band γ being discovered previously on pristine FeTe, and clearly here this band appears after the growth of 0.5 QL Bi_2Te_3, leading us to speculate that it may belong to Bi_2Te_3. Then we find this band is similar to the free-electron-like band in 1 QL Bi_2Te_3 reported by Li *et al.* in 2010.[24] To confirm our speculation, we continued the deposition of Bi_2Te_3 and acquired the band structure from the surface of 2 QLs Bi_2Te_3/FeTe, as shown in Fig. 2(f), in which a clear Dirac cone shows up below the Fermi surface, consistent with Li's results.[24] Therefore, we can confirm that this heterojunction is of good quality both in crystal structure and band structure, which is suitable for further study about edge modes.

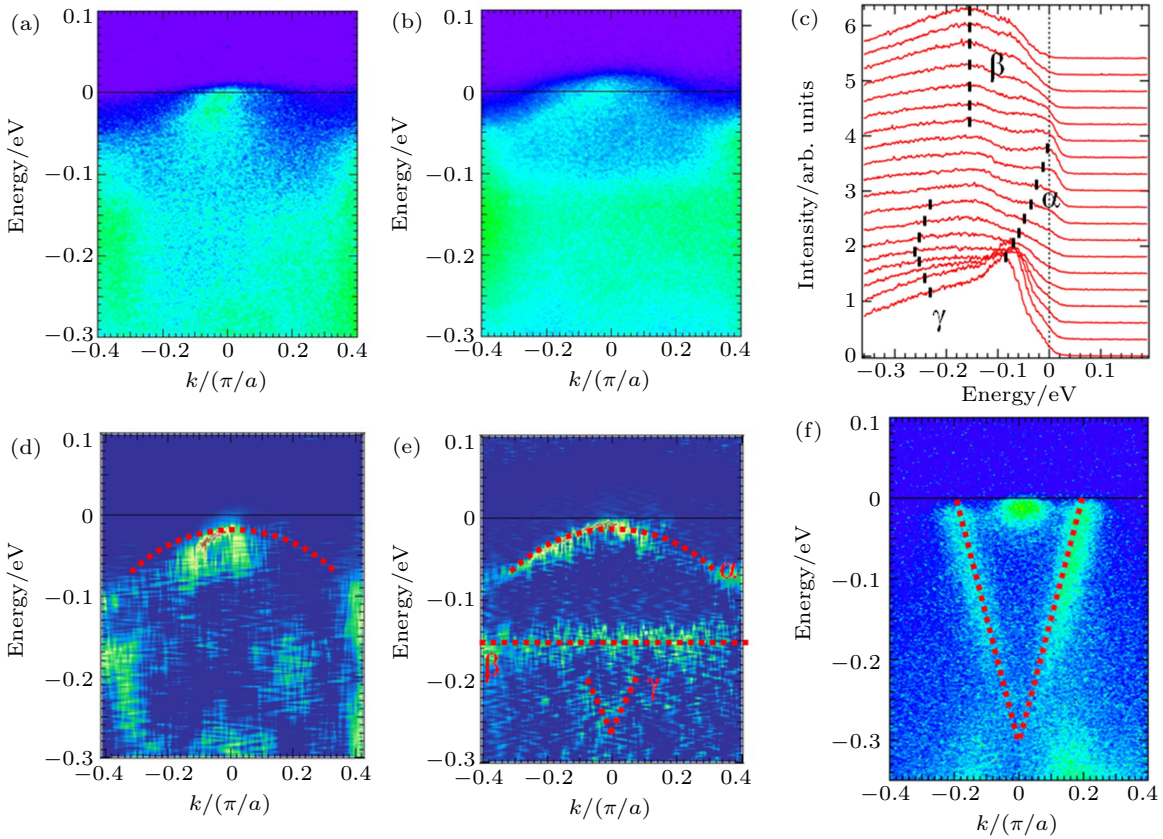


Fig. 2. (a), (b) Photoemission intensity of the cut along the Γ–M direction of FeTe acquired on pure FeTe and 0.5 QL Bi_2Te_3/FeTe heterostructure, respectively. (c) Plot of EDCs of (b). (d), (e) Differential intensity maps of (a) and (b). (f) Photoemission intensity of the cut along the Γ–K direction of Bi_2Te_3 on 2 QLs Bi_2Te_3/FeTe sample.

3.3. Robust superconductivity on Bi_2Te_3 islands

After the electronic structure is confirmed by ARPES, we focused our investigation on the topographic and electronic properties of 0.5 QL Bi_2Te_3/FeTe using STM. Figure 3(a) is a topographic image, giving a representative landscape we have observed. It can be seen that several Bi_2Te_3 islands with different sizes grow and extend from the FeTe terrace (typical growth behavior of step-flow epitaxy). Representative dI/dV spectra acquired from these islands are shown in Fig. 3(b), where a superconducting gap of $\Delta = 2.3$ meV can be extracted. Although the exact shape of each spectrum varies a bit on different islands (I to III) shown in Fig. 3(b), the two coherence peaks consistently show up, where a gap of around ± 2.3 meV with some variations can be observed in all spectra. The fixed energy gap on the islands is consistent with our previous STS on the large plateau of Bi_2Te_3 which shows transport evidencing superconductivity of $T_c = 13$ K.[19] Therefore, we conclude that the superconductivity is also well developed on all these Bi_2Te_3 islands, indicating that the superconductivity is robust and immune to the variation of lateral size of Bi_2Te_3. By applying the pulse to the tip, the tip state can be changed (depending on the state of the apex atom on the tip). We also probed the gap dependence on the tip state as shown in Fig. 3(d), obtained over position IV on the island shown in Fig. 3(c), showing that the superconducting gap's magnitude (2.3 meV) is robust against the variation of probing conditions.

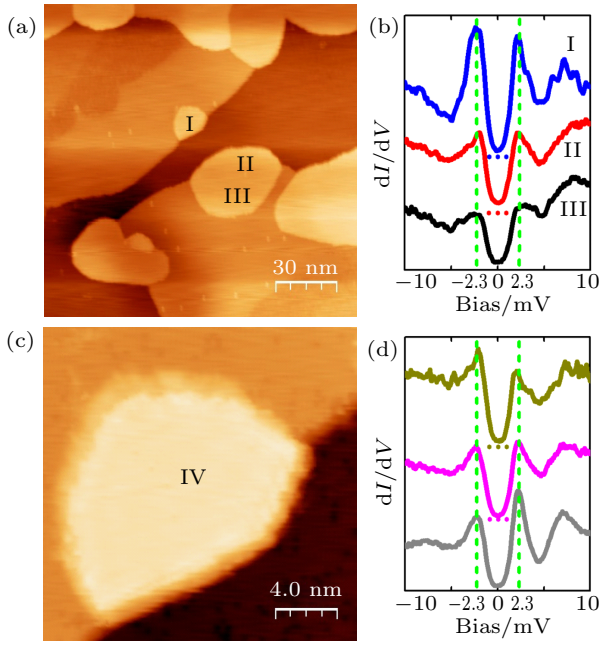


Fig. 3. (a) An STM image of different sizes of 1 QL Bi_2Te_3 islands on the FeTe terrace. (150×150 nm^2, $V_{Bias} = 200$ mV, $I_{Tunnel} = 50$ pA). (b) STS curves taken over different positions on different size Bi_2Te_3 islands with Roman numbers indicating their positions (set point: $V_{Bias} = 200$ mV, $I_{Tunnel} = 50$ pA, modulation voltage: $\Delta V = 300$ μV). (c) Zoom in image of an island in (a). (20×20 nm^2, $V_{Bias} = 200$ mV, $I_{Tunnel} = 50$ pA). (d) STS curves acquired over position IV in (c) under different tip states (set point: $V_{Bias} = 200$ mV, $I_{Tunnel} = 50$ pA, modulation voltage: $\Delta V = 300$ μV).

It is worth noting that the islands being studied all have dimensions larger than the in-plane coherent length of superconductivity, which is around 5 nm,[18] thus, we do not expect any fluctuation on the superconducting Bi_2Te_3 islands due to the quantum confinement effect here.

3.4. Probing the topological edge states

In order to get an insight into the property of these superconductive Bi_2Te_3 islands, further detailed experiments were performed over one island's edge. Figure 4(a) is a zoom in STM image showing the edge from a Bi_2Te_3 island to the FeTe terrace. From our previous studies,[19] Bi_2Te_3 starts to grow and extend from the terrace of FeTe through vdW epitaxy. The heights of one unit-cell of FeTe and one QL of Bi_2Te_3 are about 0.6 nm and 1.0 nm. In Fig. 4(a), the height differences of the edge (h_e) between the Bi_2Te_3 island and the top (right) FeTe terraces are around 0.4 nm (top edge) and 1.0 nm (right edge), respectively. Thus, it shows that the Bi_2Te_3 island grows from the top FeTe terrace, and the top edge ($h_e = 0.4$ nm) is the step between one QL Bi_2Te_3 and one unit cell FeTe terrace, whereas the right edge ($h_e = 1.0$ nm) is the step between the on-top one QL Bi_2Te_3 and the underlying FeTe terrace. Afterwards, we acquired differential conductance mapping over Fig. 4(a) under different biases (−0.5 meV, 0.5 meV, and 1.5 meV), as shown in Figs. 4(b)–4(d). For low bias voltage near the Fermi level in Figs. 4(b) and 4(c), we can find obvious brightness contrast within the Bi_2Te_3 island, where a bright belt lies along the edge of both steps (the top and the right). This indicates that the in-gap local density of states (LDOS) at this energy of the area along the edge is higher than that of the inner area of the island. Whereas for high bias at 1.5 meV (near the coherence peak) in Fig. 4(d), this brightness contrast disappears.

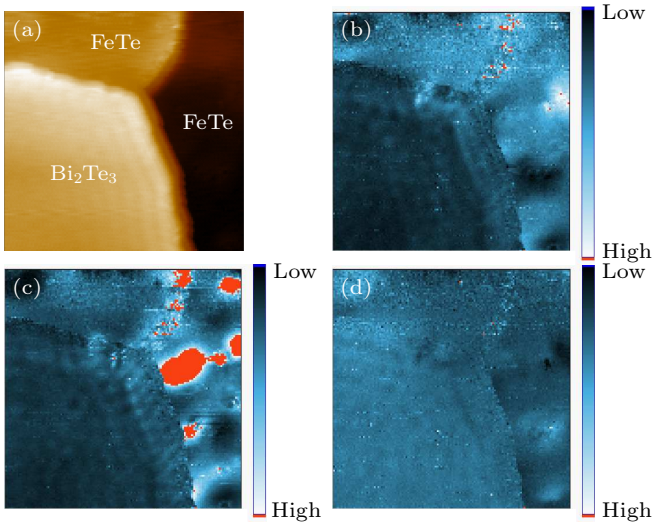


Fig. 4. (a) A zoom in STM image showing the edge of a 1 QL Bi_2Te_3 island (32×32 nm^2, $V_{Bias} = 2.5$ mV, $I_{Tunnel} = 50$ pA). (b)–(d) dI/dV mappings over (a) at 0.5 mV, −0.5 mV, and 1.5 mV, respectively (32×32 nm^2, set points: $V_{Bias} = 2.5$ mV, $I_{Tunnel} = 50$ pA, modulation voltage: $\Delta V = 300$ μV).

To get detailed information about this brightness contrast along the edge, we acquired these spectra on atoms one by one, marked by the red dots across the edge ($h_e = 0.4$ nm) as shown in the atomic resolution image Fig. 5(a). Six spectra taken over the FeTe terrace are shown in Fig. 5(b), where they display no clear coherence peaks nearby ± 2.3 meV in these spectra, showing that the superconductivity is well confined within the Bi_2Te_3 island. The eight spectra acquired on the Bi_2Te_3 island are shown in Fig. 5(c), in which the coherence peaks of the spectra are at around the same positions ± 2.3 meV, however, the LDOS near the Fermi energy increases as the position approaching the edge. To make this variation clearer, we compared the zero-bias conductance (ZBC) of each spectrum from Figs. 5(b) and 5(c) and plotted them in Fig. 5(d). We can see that the ZBC of Bi_2Te_3 near the edge is obviously higher than that at the area far away from the edge. Furthermore, if we subtract the three spectra near the edge from Fig. 5(c) by the most inner spectrum No. 1, as shown in Fig. 5(e), it can be noticed that the LDOS at the area near the edge is higher within the gap, not just at the zero energy. This result indicates the possible topological edge states near the zero-bias existing on the edge of this Bi_2Te_3 island, as being indicated in the differential conductance mapping in Fig. 4.

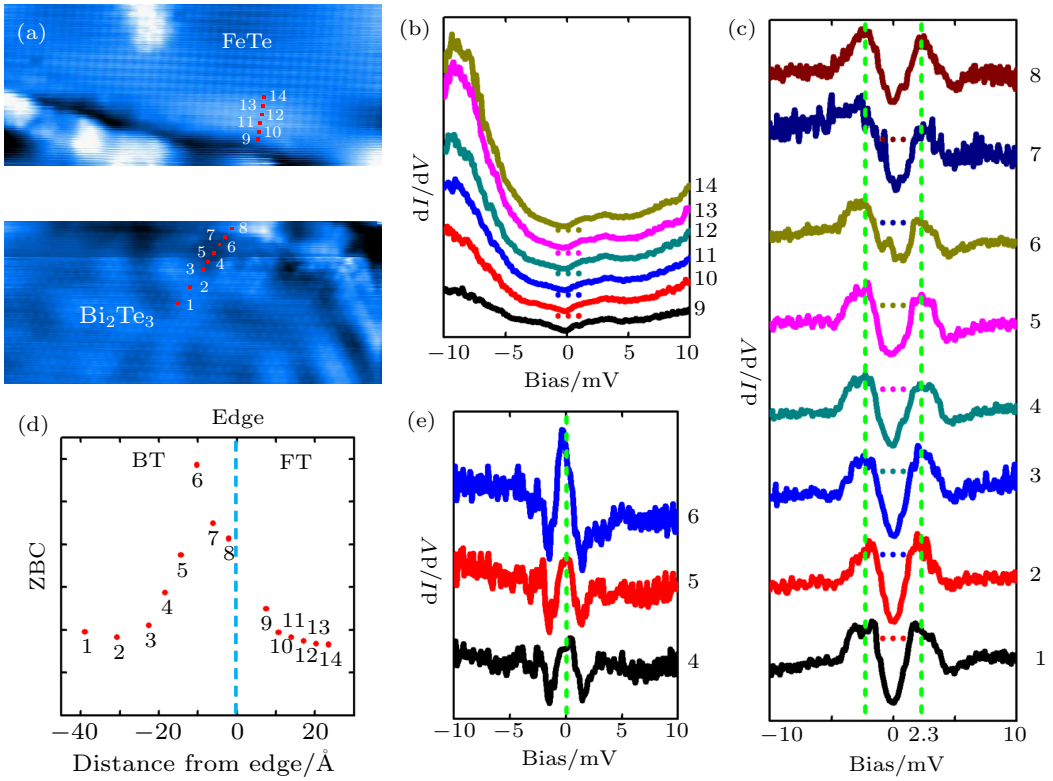


Fig. 5. (a) Zoom in atomic resolution STM images showing the top edge of the Bi_2Te_3 island in Fig. 4(a) between the Bi_2Te_3 island (bottom) and the FeTe terrace (top), respectively. Red points with numbers indicate positions where STS curves were taken (15×15 nm^2, $V_{Bias} = 10$ mV, $I_{Tunnel} = 1.5$ nA). (b) and (c) STS curves taken on the labeled positions in (a) on the FeTe terrace and the Bi_2Te_3 island (set points: $V_{Bias} = 10$ mV, $I_{Tunnel} = 1.5$ nA, modulation voltage: $\Delta V = 300$ μV). All spectra are offset vertically for clarity with dotted lines indicating the 0 position before the offset. (d) ZBC of the spectrum in (b) and (c) vs. distance from the edge. Blue line indicates the edge position. Red numbers indicate spectra positions. Dashed lines below each spectrum indicate the respective zero dI/dV value. (e) STS spectra Nos. 4–6, taken on the Bi_2Te_3 island in (c) after the subtraction of the most inner No. 1 spectrum.

3.5. Discussion and speculation

As being demonstrated above, we have achieved a high-quality epitaxy of 1 QL Bi_2Te_3 with robust superconductivity on the islands. The further atomic probing on the edge hosted LDOS gives us encouraging results that an increasing zero bias conductance does exist on the Bi_2Te_3 island's boundary nearby the FeTe. Summarizing above results leads us to speculate that the superconductivity of Bi_2Te_3/FeTe is likely topological, as several key elements already accumulate in our system: 1) robust superconductivity in the bulk, 2) strong spin–orbital coupling in Bi_2Te_3. Beside above factors, in our system, the strong localization of superconductivity is also a characteristic feature which is different with previous proximity induced topological superconductivity in topological insulators, which certainly may strengthen the detection of topological edge modes, as they can be well localized on the edge without strong dispersion. We have compared our edge modes' signature with previous reported results using WTe_2 sticking on $NbSe_2$,[9] and Fe islands grown on O_2 decorated Re superconductors,[12] and discovered that both our edge modes' location and strength are similar with them. Thus, based on above results, we would like to call at-

tention for the community that, the Bi_2Te_3/FeTe is indeed a platform for hunting the Majorana zero modes towards the realization of topological quantum computation.

Before the conclusion, we also would like to point out two key experiment concerns important for the future of exploration. As we already emphasized, our sample was grown via the MBE using step-flow epitaxy method, thus, most of the Bi_2Te_3 islands have asymmetric boundaries as one connecting the FeTe directly, and the other is directly above the FeTe. We even have found some Bi_2Te_3 which is lower than the horizontal level of FeTe as shown in the supporting materials, which shows partial edge states near the boundary as shown in the supporting materials. Till now, we still cannot tell the impact of FeTe's connection on the edge modes, as it requires more systematic research by careful selection of specimens, however, we believe that the atomic scale precision on the probing of LDOS is important for resolving above concern. The second experimental concern is about the lateral size of the Bi_2Te_3 island. As we have reported in the previous study, on the boundary of large Bi_2Te_3 terrace (~ 10000 nm^2), we did not find the obvious signature of edge modes, which certainly raises the issue of size (Bi_2Te_3 island) dependent behavior of edge modes in this system. We have found that, in Xiaoyu Chen's work,[25] they also observed such effect on probing the zero modes on Bi island grown on FeTeSe. Quantum size effects in small islands may be a reasonable explanation. But the introduce of quantum size effects also can modulate the superconductivity.[7] Although the superconducting gap observed on small Bi_2Te_3 islands (± 2.3 meV) is a little smaller than that observed on large Bi_2Te_3 terrace (± 2.5 meV),[19] the spectra acquired on Bi_2Te_3 islands of different sizes have roughly the same shape and the coherence peaks stand on the same energy. The superconductivity shows great robustness and the difference of gap size is more likely due to the intrinsic electronic properties of FeTe. Thus, it is still an open issue and we believe that a systematic study on the edge states dependence on size of Bi_2Te_3 is also an important direction not only for experiment, but also from the theoretic orientation.

4. Summary

We have fabricated single layer Bi_2Te_3/FeTe heterostructure with step-flow epitaxy method and studied the topological properties of this system by using ARPES and STM/STS. We observed robust superconductivity on all the Bi_2Te_3 islands regardless of the size of islands. Further investigation by STM and STS over different positions across the edge of single QL Bi_2Te_3 island revealed the existence of the topological edge state on the Bi_2Te_3 island. All the above results provide experimental evidences for the coexistence of topological edge states and superconductivity in single QL Bi_2Te_3/FeTe heterojunction, which indicates this system may be a potential topological superconductor and host Majorana zero modes.

References

[1] Nayak C, Simon S H, Stern A, Freedman M and Sarma S D 2008 *Rev. Mod. Phys.* **80** 1083
[2] Hasan M Z and Kane C L 2010 *Rev. Mod. Phys.* **82** 3045
[3] Qi X L and Zhang S C 2011 *Rev. Mod. Phys.* **83** 1057
[4] Chen C, Jiang K, Zhang Y, Liu C, Liu Y, Wang Z and Wang J 2020 *Nat. Phys.* **16** 536
[5] Liu C, Chen C, Liu X, Wang Z, Liu Y, Ye S, Wang Z, Hu J and Wang J 2020 *Sci. Adv.* **6** eaax7547
[6] Nishio T, Ono M and Eguchi T 2006 *Appl. Phys. Lett.* **88** 113115
[7] Nishio T, An T, Nomura A, Miyachi K, Eguchi T, Sakata H, Lin S, Hayashi N, Nakai N, Machida M and Hasegawa Y 2008 *Phys. Rev. Lett.* **101** 167001
[8] Sun H H, Wang M X, Zhu F, Wang G Y, Ma H Y, Xu Z A, Liao Q, Lu Y, Gao C L, Li Y Y, Liu C, Qian D, Guan D and Jia J F 2017 *Nano Lett.* **17** 3035
[9] Lüpke F, Waters D, Barrera S C, Widom M, Mandrus D G, Yan J, Feenstra R M and Hunt B M 2020 *Nat. Phys.* **16** 526
[10] Wang A Q, Li C Z, Li C, Liao Z M, Brinkman A and Yu D P 2018 *Phys. Rev. Lett.* **121** 237701
[11] Li C Z, Wang A Q, Li C, Zheng W Z, Brinkman A, Yu D P and Liao Z M 2020 *Phys. Rev. Lett.* **124** 156601
[12] Palacio-Morales A, Mascot E, Cocklin S, Kim H, Rachel S, Morr D K and Wiesendanger R 2019 *Sci. Adv.* **5** eaav6600
[13] Nadj-Perge S, Drozdov I K, Li J, Chen H, Jeon S, Seo J, MacDonald A H, Bernevig B A and Yazdani A 2014 *Science* **346** 602
[14] Ruby M, Heinrich B W, Peng Y, Oppen F and Franke K J 2017 *Nano Lett.* **17** 4473
[15] Mizuguchi Y, Tomioka F, Tsuda S, Yamaguchi T and Takano Y 2009 *Appl. Phys. Lett.* **94** 012503
[16] Li F, Ding H, Tang C, Peng J, Zhang Q, Zhang W, Zhou G, Zhang D, Song C L, He K, Ji S, Chen X, Gu L, Wang L, Ma X C and Xue Q K 2015 *Phys. Rev. B* **91** 220503
[17] Wang G, He Q L, He H T, Liu H C, He M, Wang J N, Lortz R, Wong G K L and Sou I K 2014 *Cryst. Growth.* **14** 3370
[18] He Q L, Liu H, He M, Lai Y H, He H, Wang G, Law K T, Lortz R, Wang J and Sou I K 2014 *Nat. Commun.* **5** 4247
[19] Qin H, Guo B, Wang L, Zhang M, Xu B, Shi K, Pan T, Zhou L, Qiu Y, Xi B, Sou I K, Yu D, Chen W Q, He H, Ye F, Mei J W and Wang G 2020 *Nano Lett.* **20** 3160
[20] Owada K, Nakayama K, Tsubono R, Shigekawa K, Sugawara K, Takahashi T and Sato T 2019 *Phys. Rev. B* **100** 064518
[21] Koma A 1992 *Thin Solid Films* **216** 72
[22] Xia Y, Qian D, Wray L, Hsieh D, Chen G F, Luo J L, Wang N L and Hasan M Z 2009 *Phys. Rev. Lett.* **103** 037002
[23] Liu Z K, He R H, Lu D H, Yi M, Chen Y L, Hashimoto M, Moore R G, Mo S K, Nowadnick E A, Hu J, Liu T J, Mao Z Q, Devereaux T P, Hussain Z and Shen Z X 2013 *Phys. Rev. Lett.* **110** 037003
[24] Li Y Y, Wang G, Zhu X G, Liu M H, Ye C, Chen X, Wang Y Y, He K, Wang L L, Ma X C, Zhang H J, Dai X, Fang Z, Xie X C, Liu Y, Qi X L, Jia J F, Zhang S C and Xue Q K 2010 *Adv. Mater.* **22** 4002
[25] Chen X, Chen M, Duan W, Yang H and Wen H H 2019 arXiv:1905.05735